LASER PROCESSING OF MATERIALS

Edited by

K. Mukherjee and J. Mazumder

CONFERENCE PROCEEDINGS

The Metallurgical Society of AIME

LASER PROCESSING OF MATERIALS

Proceedings of a symposium
sponsored by the Physical Metallurgy
and Solidification Committees of The
Metallurgical Society of AIME,
held at the 113th AIME Annual
Meeting, Los Angeles, California,
February 26 - March 1, 1984

Edited by
K. Mukherjee
Michigan State University
East Lansing, Michigan
and
J. Mazumder
University of Illinois
Urbana-Champaign
Urbana, Illinois

A Publication of The Metallurgical Society of AIME

Library of Congress Cataloging in Publication Data
Main Entry under title:

Laser processing of materials.

Includes indexes.
1. Lasers--Industrial applications--Congresses.
2. Materials--Effect of radiation on--Congresses.
3. Metallurgy--Laser use in--Congresses.
I. Mukherjee, K. II. Mazumder, J. III. Metallurgical Society of AIME. Physical Metallurgy Committee. IV. Metallurgical Society of AIME. Solidification Committee. V. AIME Meeting (113th : 1984 : Los Angeles, Calf.)
TA1.673.L366 1985 669'.0028 85-7161
ISBN 0-89520-492-4

A Publication of The Metallurgical Society of AIME
420 Commonwealth Drive
Warrendale, Pennsylvania 15086
(412) 776-9000

Printed in the United States of America.
Library of Congress Catalogue Number 85-7161
ISBN NUMBER 0-89520-492-4

THE·METALLURGICAL·SOCIETY AIME

Preface

These proceedings report a symposium held at the Annual meeting of the Metallurgical Society of AIME in Los Angeles, California, February 26, March 1, 1984, to discuss further developments in the application of high-power lasers in materials processing. Emphasis is placed on both the fundamental aspects of laser-materials interaction as well as practical applications of laser as a new tool in materials processing. This symposium was a follow-up of the "Lasers in Metallurgy" symposium held at the Annual meeting of the AIME in Chicago, Illinois, February 22-26, 1981. Proceedings of that symposium has already been published by the Metallurgical Society of the AIME under the above mentioned symposium title.

The current symposium was co-sponsored by the Physical Metallurgy and Solidification Committee of the AIME. The symposium papers were divided into four categories to provide a broader base of interest. Both domestic and foreign contributions were received. An excellent attendance at the two day symposium, demonstrated a very strong interest in this developing new field of endeavor. It would appear that since the last symposium in 1981, considerable progress has been made in modeling heat flow, control of microstructure developed during laser processing and understanding fundamental mechanisms of laser-materials interaction. However, much of the applications appear to be still in the developmental state although some very practical problems, such as laser hardening of large gears etc., were shown to be technologically and economically competitive with conventional processes.

In the area of laser welding, thickness limitation still continued to be the problem but some recent ideas on narrow-gap welding of thicker sections were discussed. Attempts to weld or join metastable materials, such as metallic glasses, were discussed. Again these studies seem to pose many fundamental problems such as crack formation associated with pulse laser shock wave etc.

In summary the symposium demonstrated that many interesting problems exist in laser-materials interactions and a potential for technological innovation through laser applications in materials processing is quite high. However, further extensive research and development are needed before a large scale laser application is more widely accepted in our industrial community.

We would like to take this opportunity to thank the authors for presenting these papers. We would also like to thank the session chairmen for their effort in organizing the sessions, for stimulating technical discussions and for their participation in the round-table discussions. We would like to thank Mr. N. Dahotre and Mr. C. Wakade for their help in indexing this book. We would also like to thank Ms. Michelle Ward and Ms. Arlene Klingbiel, secretaries in the Department of Metallurgy, Mechanics and Materials Science, Michigan State University for technical support in preparation of the final manuscript of this publication.

K. Mukherjee
Department of Metallurgy,
Mechanics and Materials Science
Michigan State University
East Lansing, Michigan

J. Mazumder
Department of Mechanical Engineering
University of Illinois
Urbana, Illinois

January 1985

Table of Contents

SURFACE MODIFICATION-II

Transport Phenomena Theory for Laser Processing

AN AXIS-SYMMETRY MODEL FOR CONVECTION IN A LASER MELTED POOL

by

C. Chan, J. Mazumder, and M. M. Chen

Department of Mechanical and
Industrial Engineering
University of Illinois at Urbana-Champaign
1206 West Green Street
Urbana, IL 61801

An axis-symmetry model of the fluid flow and heat transfer of laser melted pool is developed. The model corresponds physically to a stationary laser source. Non-dimensional form of the governing equations are derived. Four dimensionless parameters arise from the non-dimensionalization, namely, Peclet number (Pe), Prandtl number (Pr), Dimensionless melting temperature (T_m^*), and Radiation factor (RF). Their effects and significances are discussed. Numerical solutions for some low melting point metals are obtained. The solid liquid interface, which is not known a priori, is solved. Quantitative effects of the dimensionless parameters on pool shape are obtained. In order to understand the process in a more physical sense, the effects on pool shape due to process parameters, total power (Q) and beam radius (r_0), are also presented. In the presence of the flow field, the heat transfer becomes convection dominated. Its effect on isotherms within the molten pool is discussed.

Introduction

It has been pointed out by a number of researchers (1-18) that convection plays a major role in arc, laser, and electron beam weld pools. Convection is the single most important fact influencing the geometry of the pool in luding pool shape, undercut, and ripples, and can result in defects such as variable penetration, porosity, and lack of fusion. Convection is also primarily responsible for mixing, and, therefore affects the composition of the weld pool. The heat transfer, and thus the cooling rate, is greatly enhanced in the presence of convection (17). This in turn will affect the microstructure. The homogeneity of solute redistribution during Laser Surface Alloying (LSA), as reported by Chande, and Mazumder (7), can only be explained by the presence of convection current.

Surface tension driven flow has been identified to be responsible for the convection within the molten pool. While most of the work to date has been qualitative, a quantitative understanding of the effect of convection on pool shape and mixing is of importance. Anthony and Cline (6) did an analysis on the surface tension driven flow within the molten pool. It is essentially an one-dimensional problem and the flow field thus obtained is not coupled to the energy equation. Therefore, no additional information is obtained as far as the heat transfer process is concerned. Szekely, et al. (31) developed a two-dimensional convection model. Buoyancy, electromagnetic and surface tension forces are considered. However, they have assumed the profile of the solid-liquid interface, as pointed out earlier, the solid-liquid interface is not known a priori. It is part of the problem to be solved. In fact, the solid-liquid interface, i.e. the pool shape, is one of the informations that is of great interest. A two-dimensional transient model for laser surface melted pool was first developed by Chan, Mazumder and Chen (10,11). It is shown (10,11) that surface tension is responsible for the fluid flow and convection. The cooling rate at the edge of the pool is found to be higher than that at the bottom of the pool below the centerline, which agrees with the experimental findings that the microstructure is finer at the edge of the pool than at the bottom of the pool. Depending on the Prandtl number (i.e. material) and surface tension number, the shape of the molten region as well as the cooling rate changes. It is also predicted that the recirculating velocity is of one or two order of magnitude higher than that of the scanning speed.

To have a better understanding, a three-dimensional model is developed. In view of the fact that the scanning speed is much smaller than the recirculating velocity, an asymptotic solution is attempted. The solution to the three-dimensional case is decomposed into two parts. This is possible because of the fact that the recirculating velocity is much higher than the scanning speed, so that the heat transfer within the molten pool is dominated by the recirculating flow. Furthermore, the Peclet number (Pe) based on the scanning speed is of order one, implying that the three-dimensional solution will be closed to the axis-symmetry case. As the first step to the three-dimensional case, solution to the axis-symmetry case is obtained. This physically corresponds to the stationary spot source.

In this paper, the convection heat transfer and fluid flow in a stationary laser melted pool is analyzed. Non-dimensional form of the governing equations are derived. Four dimensionless parameters are identified and each governs different characteristics of the problem. Numerical solution is obtained. The solid-liquid interface, which is not known a priori, is solved by an iterative scheme. Quantitative effects of various dimensionless parameters and process parameters on pool shape are presented and discussed. The effect of convection on the isotherm within the molten pool due to the convection current is presented and discussed.

Physics of the Process

A three-dimensional analysis is presented, modeling a circular source laser beam having a uniform power distribution striking the surface of an opaque material of width W, thickness D, and length L (Fig. 1). Some of the incident radiation is reflected while the rest is absorbed. The heat absorbed developed a molten pool. Owing to the high temperature gradient on the surface in the radial direction, the surface tension gradient is developed. It is this mechanism that drives the flow. As the flow develops, energy transfer mechanism becomes a convection problem with the flow driven by the surface tension gradient.

The basic assumptions are as follows.

1. All the properties of the liquid metal and solid metal are constant, independent of temperature (except the surface tension). This allows simplifications of the model; however, variable properties can be treated with slight modifications. The dependence of surface tension on temperature, the driving force of the flow, is assumed to be linear.
2. Thermal conductivity is assumed to be the same for both liquid and solid phases. Such an assumption does not change the physics but simplify the computation.
3. Surface of the melt pool is assumed to be flat, to simplify the surface boundary condition, and hence, surface rippling is not considered.
4. Because of the fact that the heat affected zone is very localized, a semi-infinite domain is assumed.
5. A grey body radiative heat loss is assumed.

Mathematical Formulation

The appropriate governing equations are:

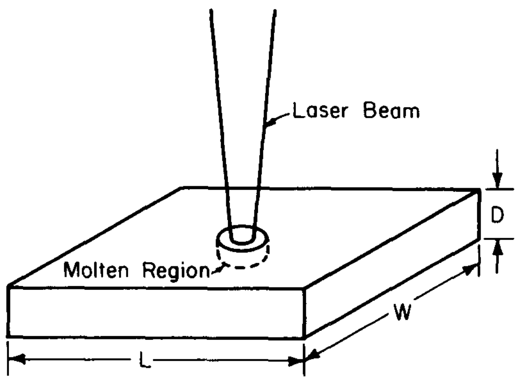

Figure 1 Schematic Diagram of the Model

The continuity equation,

$$\underline{\nabla} \cdot \underline{u} = 0 \tag{1}$$

the momentum equation,

$$\frac{\partial}{\partial t} \underline{u} + (\underline{u} \cdot \underline{\nabla}) \underline{u} = - \frac{\nabla P}{\rho} + \nu \nabla^2 \underline{u} \tag{2}$$

and the energy equation,

$$\frac{\partial}{\partial t} T + (\underline{u} \cdot \underline{\nabla}) T = \kappa \nabla^2 T \tag{3}$$

and subject to the boundary conditions.
At the surface,

$$z = 0,\ u_z = 0,\ \mu \frac{\partial u_r}{\partial z} = -\gamma \frac{\partial T}{\partial r}$$

$$k \frac{\partial T}{\partial z} = \begin{cases} -q + \varepsilon \sigma T^4, & r < r_o \\ \varepsilon \sigma T^4 & r > r_o \end{cases} \tag{4}$$

at the solid-liquid interface,

$$f(r,z) = C;\ u_r = u_z = 0,\ T = T_m \tag{5}$$

and finally,

$$\text{as } r,z \rightarrow \infty,\ T = T_\infty \tag{6}$$

It is important to point out that $f(r,z) = C$ defines the solid-liquid interface. It is part of the problem to be solved. This type of problem is generally known as the Stefan problem in the literature. An iterative scheme is developed to solve for the interface.

Introducing the dimensionless variables as follows:

$$r^* = \frac{r}{r_o},\quad z^* = \frac{z}{z_o},\ u_r^* = \frac{u_r}{u_c},\ u_z^* = \frac{u_z}{u_c},\ \rho^* = \frac{P}{\rho u_c^2},\ T^* = \frac{T-T_\infty}{q r_o / k},$$

where

$$u_c = \frac{\gamma' q r_o}{k \mu}$$

and because of the symmetry in θ-direction. The governing equations become

$$\frac{\partial u_r^*}{\partial r^*} + \frac{u_r^*}{r^*} + \frac{\partial u_z^*}{\partial z^*} = 0$$

$$U_r^* \frac{\partial u_r^*}{\partial r^*} + u_z^* \frac{\partial u_z^*}{\partial z^*} = - \frac{\partial P^*}{\partial r^*} + \frac{Pr}{Pe} \left(\frac{1}{r^*} \frac{\partial}{\partial r^*} r^* \frac{\partial u_r^*}{\partial r^*} + \frac{\partial^2 u_r^*}{\partial z^{*2}} - \frac{u_r^*}{r^{*2}}\right)$$

$$u_r^* \frac{\partial u_z^*}{\partial r^*} + u_z^* \frac{\partial u_z^*}{\partial z^*} = - \frac{\partial P^*}{\partial z^*} + \frac{Pr}{Pe} \left(\frac{1}{r^*} \frac{\partial}{\partial r^*} r^* \frac{\partial u_z^*}{\partial r^*} + \frac{\partial^2 u_z^*}{\partial z^{*2}}\right)$$

$$u_r^* \frac{\partial T^*}{\partial r^*} + u_z^* \frac{\partial T^*}{\partial z^*} = \frac{1}{Pe}\left(\frac{1}{\partial r^*} r^* \frac{\partial T^*}{\partial r^*} + \frac{\partial^2 T^*}{\partial z^{*2}}\right)$$

and the boundary conditions become,

$$z^* = 0;\ u_z^* = 0,\ \frac{\partial u_r^*}{\partial z^*} = -\frac{\partial T^*}{\partial r^*}$$

$$\frac{\partial T^*}{\partial r^*} = \begin{cases} -1 + RF \cdot T^{*4} & , r^* < 1 \\ RF\ T^{*4} & , r^* > 1 \end{cases}$$

at the solid-liquid interface

$$f^*\ (r^*,z^*) = C;\ u_r^* = u_z^* = 0,\ T^* = T_m^*,$$

and as $r^*, z^* \to \infty$, $T^* = 0$

where $$Pe = \frac{u_c r_o}{\kappa},\ Pr = \frac{\nu}{\kappa},$$

$$T_m^* = \frac{T_m - T_\infty}{q\ r_o/k},\ \text{and } RF = \varepsilon\sigma\,\frac{k}{q}\left(\frac{q r_o}{k}\right)^4$$

are the dimensionless parameters. The Peclet number that we have is also known as Marangoni number.

In order to gain more physical insight of the various dimensionless parameters, they are further broken down. First, it is easy to note that the heat flux,

$$q = \frac{Q}{\pi\ r_o^2}$$

where Q is the total power from the laser and r_o is the beam radius. The dimensionless parameters, in terms of these process parameters, become

$$Pe = \frac{\gamma' Q}{\pi k \mu \kappa},$$

$$T_m^* = T_m - T_\infty\ k\ \pi\,\frac{r_o}{Q},$$

$$RF = \varepsilon\sigma\,\frac{1}{(\pi k)^3}\left(\frac{Q^3}{r_o^2}\right),$$

while the Prandtl number, which is a material property, remains unchanged. Peclet number bases on the surface tension velocity, as pointed out earlier, is also known as the Marangoni number. It governs the thermocapillary convection, and thus the pool shape. The higher the Peclet number, the higher the convection. The Prandtl number is the ratio of momentum diffusion and energy diffusion. The dimensionless melting temperature defines the solid-liquid interface. The radiation factor governs the heat loss on the surface due to radiation. The order of magnitude of each of the above dimensionless parameter is estimated for some low melting point metals to give a better understanding (Table I).

Table I Order of Magnitude of the Dimensionless Parameter for Low Melting Point Metals

	Tin	Bismuth	Zinc
Pe	$10 - 10^3$	$10 - 10^3$	$10 - 10^3$
Pr	0.015	0.02	0.03
T_m^*	$10^{-2} - 10^{-1}$	$10^{-2} - 10^{-1}$	$10^{-2} - 10^{-1}$
RF	$1 - 10^2$	$1 - 10^2$	$1 - 10^2$

Results and Discussions

A standard Alternating Direction Iterative (ADI) method is employed to solve the governing equations. Numerical solutions for seven cases have been obtained. The values of the governing parameters are tabulated in Table II. The dimensionless temperature on the surface in the radial direction for Case (3) is plotted in Fig. 2. The maximum temperature occurs at the center of the pool and decreases in the radial direction. The temperature gradient is always negative and it attains its maximum magnitude at the edge of the laser beam ($r^* = 1.0$). Because of the fact that surface tension is a decreasing function of temperature for most of the metals, the molten liquid is pulled to the side. Recirculation flow is thus set up, when the molten metal hits the edge of the pool.

Table II The Numerical Values of the Dimensionless Parameters of Various Cases

	1	2	3	4	5	6	7
Pe	100	200	500	50	10	50	100
Pr	0.1	0.1	0.1	0.05	0.01	0.1	0.1
T^*_m	0.05	0.05	0.05	0.05	0.05	0.1	0.1
RF	100	100	100	100	100	12.5	2.5

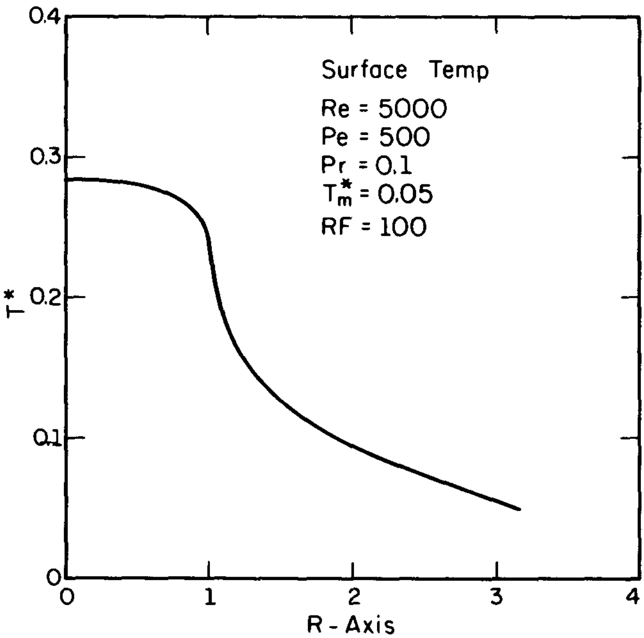

Figure 2 Surface Temperature of the Molten Pool in the Radial Direction

Effect of Convection

The velocity field within the molten pool in the r-z plane for Case 3 is presented in Fig. 3. A mirror image along the vertical axis r=0 will complete the molten pool. The recirculating pattern of the flow field can be observed clearly. The very existence of the flow field changes the mechanism of heat transfer. It tends to bring the higher temperature fluid on the surface right underneath the beam sideway. This in turn melts down the solid at the edge of the molten pool more, creating a wider pool. Because of the conservation of energy, the size of the molten pool has to remain unchanged with or without convection. As a result, the molten pool becomes shallower. This effect is shown clearly in Fig. 4, where the solid-liquid interfaces for both pure conduction and convection are plotted. The effect of an increase in Peclet number on the pool shape can also be observed. Peclet number is a measure of the convection. An increase in Peclet number implies an increase in the amount of heat being brought sideway. Consequently, the molten pool becomes wider and wider. The aspect ratio (width by depth ratio) for different Peclet numbers are tabulated in Table III. The changes are quite large, up to a 45% increase. The corresponding Peclet number is 500 which is very moderate. For the case of steel and aluminum, the Peclet number will go up to $10^5 \sim 10^6$. The effects on changing the pool shape can be expected to be much greater.

Effect of Prandtl Number

The effect of changing the Prandtl number is also studied. Prandtl number is the ratio of the momentum diffusion to heat diffusion. To study its effect, one way is to keep the momentum diffusion constant and vary only the heat diffusion. This corresponds to keeping the Reynold number (Re = Pe/Pr) constant and change Pr and Pe. This in some sense implies that the flow field is being kept the same, while changing the thermal diffusion. Although caution must be exercised because of the complexity of the process due to the coupling of the energy and momentum equations. An increase in Prandtl number with the Reynold number being kept constant will

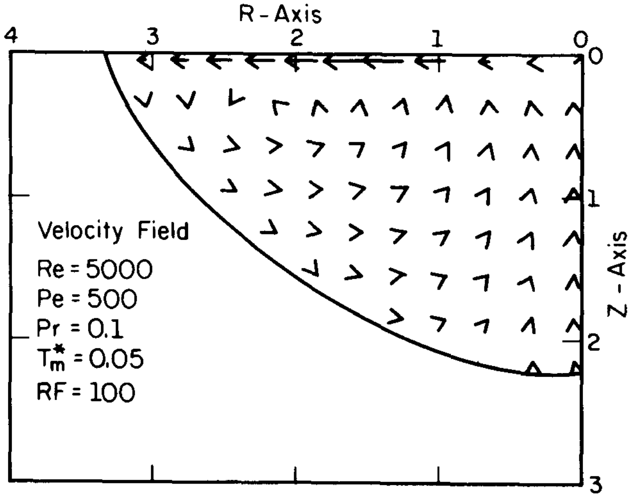

Figure 3 Convective Current within the Molten Region

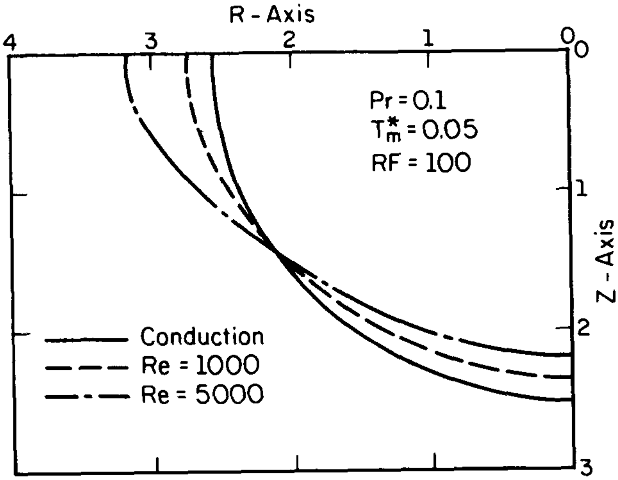

Figure 4 Solid-Liquid Interface (Shape of the Molten Pool) for various Reynolds Number

Table III Aspect Ratio (width by depth) for Different Pe numbers

$Pr = 0.1, \quad T_m^* = 0.05, \quad RF = 100$

	width/depth
Pure Conduction	2.0
Pe = 100	2.3
= 200	2.5
= 500	2.9

increase the Peclet number, and hence the convective heat transfer. The aspect ratio will therefore increase with the Prandtl number (Table IV).

Effect of Total Power and Beam Radius

The effect of the process parameters on the pool shape is also investigated. Cases 1 and 6 in Table II correspond to the case of keeping the beam radius constant while changing the total power. If the beam radius is fixed, the input heat flux will increase with the total power. Higher the heat flux, higher the penetration. The aspect ratio will therefore decrease with increasing total power (Table V). Cases 1 and 7 in Table II on the other hand represents the case of keeping the total power constant while varying the beam radius. The heat flux is inversely proportional to r_o^2. The penetration will decrease with increasing beam radius, and thus increases the aspect ratio (Table VI).

Table IV Aspect Ratio for Different Pr Numbers

Re = 1000, T_m = 0.05, RF = 100

Pr	width/depth
0.01	2.1
0.05	2.2
0.1	2.3

Table V Aspect Ratio for Changing Total While keeping r_o constant

Pr = 0.1

	width/depth
Pe = 100 T_m^* = 0.05 RF = 100	2.3
Pe = 50 T_m^* = 0.1 RF = 12.5	2.36

Table VI Aspect Ratio for Changing Mean Radius While keeping Total Power Constant

Pr = 0.1

	width/depth
Pe = 100 T_m^* = 0.05 RF = 100	2.3
Pe = 100 T_m^* = 0.1 RF = 25	2.46